UV-Enhanced removal of enrofloxacin in water using oyster shell-derived CaO-ZnO composite

Mastavioni Sihombing[1], *Nurfiah* Azizah[1], *Siti* Febriyanti[2], *Adithya Zulfadli* Miraza[2], *Vicky* Prajaputra[1,4*], *Nadia* Isnaini[3,4], *Sofyatuddin* Karina[1], and *M.* Riswan[1]

[1]Department of Marine Sciences, Faculty of Marine and Fisheries, Universitas Syiah Kuala, Banda Aceh 23111, Indonesia
[2]Department of Fisheries Resources Utilization, Faculty of Marine and Fisheries, Universitas Syiah Kuala, Banda Aceh 23111, Indonesia
[3]Department of Pharmacy, Universitas Syiah Kuala, Banda Aceh 23111, Indonesia
[4]ARC-PUI Nilam Aceh, Universitas Syiah Kuala, Banda Aceh 23111, Indonesia

Abstract. The contamination of aquatic environments by enrofloxacin, a commonly used veterinary antibiotic, poses serious risks to both ecosystem health and human safety. This study investigates the potential of calcium oxide-zinc oxide (CaO-ZnO) composites derived from oyster shells for the UV-enhanced degradation of enrofloxacin in water. The CaO-ZnO composites were synthesized via calcination of oyster shells mixed with zinc oxide and characterized using X-ray diffraction (XRD) to determine their mineral properties. Enrofloxacin was detected at a maximum absorption wavelength of 272 nm using UV-Vis spectroscopy. The removal efficiency of the CaO-ZnO composites was assessed at room temperature, with varying contact times (30-150 minutes) and pH levels (3, 6, and 9). The results demonstrated that the CaO-ZnO composite achieved the best performance at pH 3, with a removal efficiency of 42.87% after 150 minutes. Under UV light from sunlight, the removal efficiency was significantly enhanced, reaching 61.04% compared to 14.53% for CaO. These findings suggest that CaO-ZnO composites derived from oyster shells are promising materials for the effective UV-enhanced removal of enrofloxacin from contaminated water sources. However, further improvements are needed by optimizing additional parameters to enhance their effectiveness.

1 Introduction

The presence of pharmaceutical residues in aquatic environments, particularly enrofloxacin, has become a pressing global concern [1]. Enrofloxacin, a fluoroquinolone antibiotic, is extensively used in veterinary medicine and aquaculture due to its high efficacy against bacterial infections in livestock and fish [2]. In aquaculture, it is often administered through medicated feed or directly into aquatic systems to control bacterial outbreaks that threaten fish health and farming operations [3]. However, a substantial fraction of the administered antibiotic remains unmetabolized and is excreted in its active form, either as the parent

---

* Corresponding author: vicky_prajaputra@usk.ac.id

compound or its metabolite [4]. These residues enter aquatic ecosystems via uneaten feed, fish excreta, and untreated or inadequately treated effluents from aquaculture facilities. Their accumulation in water bodies poses significant risks due to the compound's persistence and low biodegradability, resulting in environmental contamination and potential threats to human and ecosystem health.

Adsorption is a cost-efficient and practical method for reducing the concentration of organic compounds in wastewater [5]. This technique works by capturing organic compounds on the surface of adsorbent particles, facilitated by interactions with the active sites on the adsorbent surface [6]. The effectiveness of adsorption depends largely on factors such as the surface area, the number of active sites, and the ease with which the target compounds can access the adsorbent [7, 8]. Various adsorbents have been studied for the removal of organic pollutants from waters, including beach sand [9], activated carbon [10, 11], volcanic soil [12, 13], pumice [14, 15], zeolites [16, 17], chitosan [18, 19], silica (SiO_2) [20, 21], magnetite [22, 23], bentonite [24, 25] and composite materials [26, 27]. Recently, there has been a growing emphasis on developing cost-effective, locally sourced adsorbents to enhance the sustainability and efficiency of wastewater treatment.

Oyster shells, a byproduct of fisheries rich in calcium carbonate ($CaCO_3$), are increasingly being considered as a natural adsorbent for capturing organic pollutants in wastewater [28, 29]. Their abundant availability along the coastal areas of Alue Naga (Banda Aceh) and their porous surface structure present significant potential for wastewater treatment applications. Through the calcination process, $CaCO_3$ from oyster shells can be transformed into calcium oxide (CaO), which possesses basic properties, a larger surface area, and more active sites for adsorption [30]. However, while CaO can adsorb various contaminants, its capability is limited to physical adsorption without chemically degrading pollutants, particularly complex organic compounds like antibiotics. The effectiveness of CaO as an adsorbent is also hindered by its low chemical stability and lack of photocatalytic properties, which are crucial for pollutant degradation. To address these limitations, CaO needs to be composited with semiconductor materials such as ZnO to impart photocatalytic properties capable of breaking down organic compounds in water. ZnO is a well-known semiconductor with a bandgap energy of 3.4 eV, offering antibacterial properties, chemical stability, and high efficiency for photodegradation [31]. It has been widely utilized in wastewater treatment due to its ability to decompose organic pollutants through photocatalysis. To date, no research has explored the characteristics and potential of CaO-ZnO composites derived from oyster shells as an adsorbent for enrofloxacin, leaving their adsorption capacity largely unknown. Therefore, this study will investigate the ability of these composites to remove enrofloxacin from water under UV Light.

2 Experimental

2.1 Materials

This research was conducted in the Marine Chemistry and Biotechnology Fisheries Laboratory, Faculty of Marine and Fisheries, Universitas Syiah Kuala. The primary samples, consisting of oyster shells, were collected from Alue Naga Coastal, specifically at the geographic coordinates of 5.5461° N latitude and 95.3747° E longitude. The collected samples were then rinsed with distilled water, dried at 100°C, and ground into a powder before being used as raw materials for preparing calcium oxide (CaO). All chemicals used in this experiment, including enrofloxacin ($C_{19}H_{22}FN_3O_3$), zink chloride ($ZnCl_2$), methanol (CH_3OH), hydrogen chloride (HCl), and sodium hydroxide (NaOH), were sourced from Merck and were of high-grade quality.

2.2 CaO-ZnO composite preparation

The preparation of calcium oxide (CaO) from oyster shells involved an initial cleaning and drying process to remove contaminants. The oyster shells were then calcined at 800°C for 3 hours. During this thermal treatment, the calcium carbonate ($CaCO_3$) in the oyster shells decomposed, producing CaO and releasing carbon dioxide (CO_2). A total of 2.5 g of CaO was mixed with 125 mL of H_2O and 10 mL of methanol, then stirred using a hotplate at 40ºC for 3 hours until homogeneous. While stirring, 2.5 g of $ZnCl_2$ was added and allowed to react for the specified time. After 3 hours, the CaO-$ZnCl_2$ mixture was filtered using filter paper and a vacuum pump to obtain the residue. The resulting solid was dried in an oven at 80ºC for approximately 30 minutes until a constant weight was achieved. The obtained solid powder was then calcined in a furnace at 800ºC for 3 hours to form the CaO-ZnO biocomposite. Finally, the biocomposite was characterized using XRD.

2.3 Enrofloxacin adsorption

2.3.1 Effect of contact time

An amount of 0.05 g of adsorbent was added to 10 mL of enrofloxacin solution with a concentration of 25 mg/L. The mixture was stirred for 0.5 to 2.5 hours at room temperature (30 °C). After the adsorption period, the treated solutions were centrifuged for one minute, and the final enrofloxacin concentrations were measured using a UV-Vis spectrophotometer. The adsorption efficiency (%A) and enrofloxacin uptake capacity (q_t, in mg/g) were then calculated using Equations 1 and 2, respectively.

$$\%A = \frac{(C_0 - C_t) \times 100}{C_0} \tag{1}$$

$$q_t = \frac{(C_0 - C_t) \times V}{m} \tag{2}$$

where C_0 and C_t are the initial enrofloxacin concentration (mg/L) and the enrofloxacin concentration after 't' time (mg/L), respectively; m is the mass of the adsorbent (g), and V is the total volume of the enrofloxacin solution (L).

2.3.2 Effect of pH

To evaluate the effect of pH on enrofloxacin removal, enrofloxacin solutions (25 mg/L) with pH values of 3, 6, and 9 were prepared by adjusting the pH with either HCl or NaOH. Each solution was stirred thoroughly and then allowed to stand for 2.5 hours at room temperature (30°C). After this period, the mixtures were centrifuged for one minute to separate the adsorbent particles. The enrofloxacin concentration in the resulting supernatant was measured using a UV-Vis spectrophotometer. The adsorption capacity, expressed as uptake capacity (q_t, in mg/g), was then calculated using Equation 2.

2.4 Enrofloxacin photodegradation

A total of 0.05 g of CaO-ZnO composite was mixed with 10 mL of enrofloxacin solution at the optimal concentration and pH which produced the highest adsorption capacity from the adsorption process. The mixture was stirred under UV light for 2.5 hours. After the

photodegradation process, the enrofloxacin concentration in the solution was measured using a UV-Vis spectrophotometer. The degradation efficiency of enrofloxacin using the CaO-ZnO composite was calculated using Equation 1.

3 Results and discussion

3.1 XRD analysis

The XRD results of CaO and CaO-ZnO composites are presented in Figure 1. The results revealed distinct crystallographic characteristics for each material. For CaO, the XRD diffraction pattern displayed sharp peaks at 2θ angles of approximately 8.95°, 17.90°, 27.02°, and 45.67°. Meanwhile, the CaO-ZnO composite exhibited similar peaks to those of CaO. Additionally, two new peaks were observed at 2θ angles of around 47.46° and 56.55°, which were presumed to be characteristic of ZnO. This assumption was supported by Zhang et al. [32], who reported characteristic ZnO peaks at 2θ angles of approximately 47.65° and 56.55°. These findings confirmed the successful formation of the CaO-ZnO composite.

3.2 The maximum wavelength of enrofloxacin

The maximum wavelength of the enrofloxacin solution was determined using a UV-Vis spectrophotometer, as shown in Figure 2. The wavelength was identified by recording the absorbance of the enrofloxacin solution within the range of 250 nm to 500 nm. The results revealed a maximum wavelength at 272 nm, where the enrofloxacin molecules exhibited the strongest interaction with light, producing the highest absorbance peak. This peak served as a key marker for detecting or quantifying enrofloxacin concentration, as each compound possesses a distinct absorbance profile in a specific wavelength range. Consequently, 272 nm was chosen as the optimal wavelength for enrofloxacin analysis using the UV-Vis spectrophotometer.
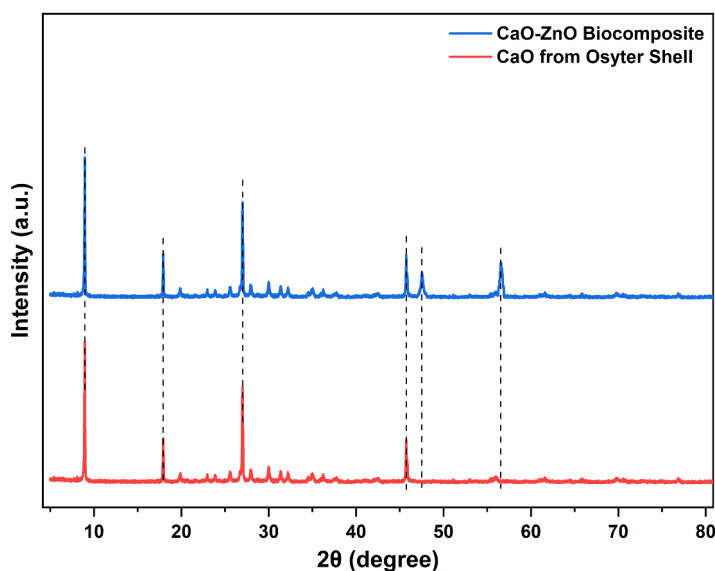

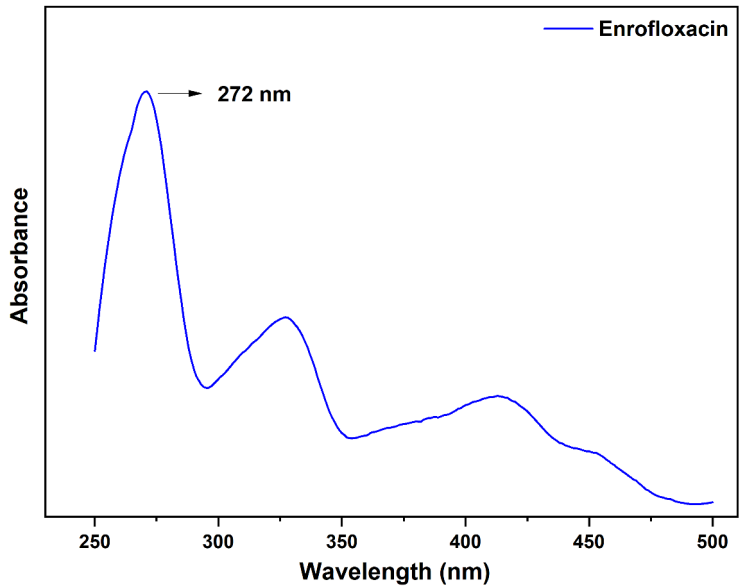**Fig. 1.** XRD spectra of CaO and CaO-ZnO biocomposite.

Fig. 2. The maximum wavelength of enrofloxacin in water.

3.3 The influence of contact time on enrofloxacin adsorption

Adsorption time is a crucial parameter influencing the adsorption process of a substance onto an adsorbent material [33]. Figure 3 illustrates the adsorption capacity of the biocomposite for enrofloxacin uptake at various contact times ranging from 30 to 150 minutes. The data revealed a rapid increase in adsorption capacity, reaching 0.94 mg/g within the first 30 minutes, indicating a high initial adsorption rate. This rapid uptake can be attributed to the abundance of active sites on the biocomposite during the initial phase of the process. The adsorption capacity continued to rise, reaching 1.21 mg/g at 60 minutes. However, after 60 minutes, the adsorption rate gradually decreased, eventually plateauing as equilibrium was approached around 120 minutes, with a final adsorption capacity of 1.25 mg/g and a percentage adsorption of 25.68%. This trend suggests that over time, the active sites on the CaO-ZnO biocomposite became saturated, limiting further adsorption.
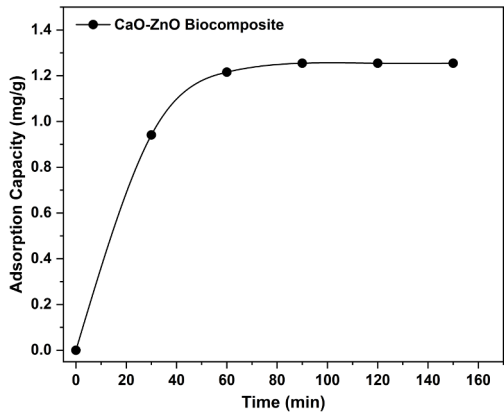

Fig. 3. Adsorption capacity of composite for enrofloxacin uptake from 0-150 minutes.

3.4 The influence of pH on enrofloxacin adsorption

Figure 4 illustrates the effect of pH on adsorption capacity of CaO-ZnO biocomposite for enrofloxacin adsorption. The results showed that the composite achieved the best performance at pH 3, with a removal efficiency of 42.87% and an adsorption capacity of 2.318 mg/g. As the pH increased, the adsorption capacity declined to 1.098 mg/g at pH 6 and 0.705 mg/g at pH 9. This behavior is attributed to the surface charge of the biocomposite, which is negatively charged due to the deprotonation of hydroxyl groups. At acidic pH, enrofloxacin molecules are positively charged due to the protonation of their amine groups, creating strong electrostatic attraction with the negatively charged biocomposite surface and significantly enhancing adsorption capacity. Conversely, at basic pH, both the biocomposite surface and enrofloxacin molecules acquire negative charges due to the deprotonation of hydroxyl and carboxyl groups, respectively, resulting in electrostatic repulsion and a reduced adsorption capacity. Thus, the higher adsorption efficiency at acidic pH is primarily driven by favorable electrostatic interactions between the biocomposite and enrofloxacin molecules.
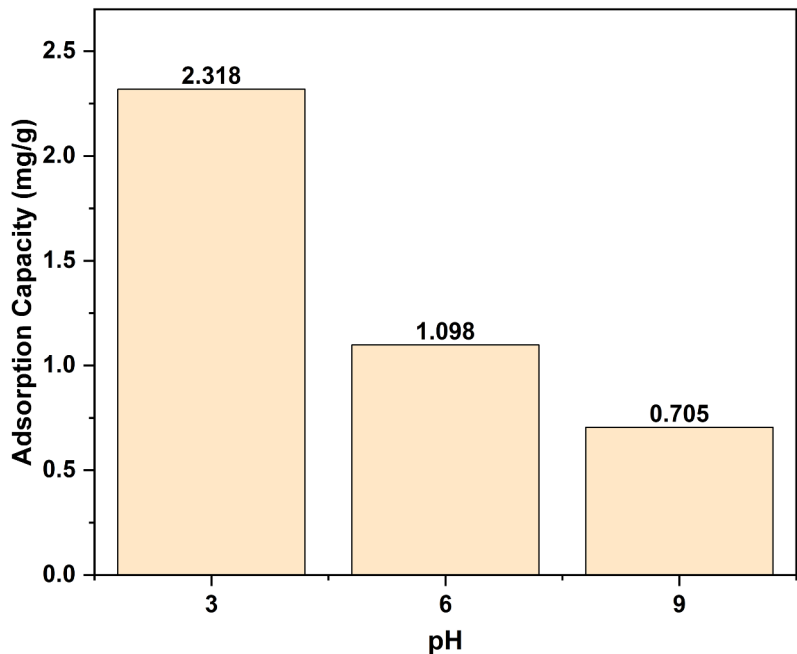

Fig. 4. Effect of pH on adsorption capacity of composite for enrofloxacin adsorption.

3.5 Enrofloxacin photodegradation

Figure 5 shows the percentage of enrofloxacin removal using CaO and CaO-ZnO biocomposites under two conditions: without UV and with UV exposure. Without UV irradiation, the CaO-ZnO biocomposite achieved a significantly higher removal efficiency (42.87%) compared to CaO (13.25%), indicating that the addition of ZnO enhanced the adsorption capacity. Under UV exposure, the removal efficiency increased for both materials, with the CaO-ZnO biocomposite reaching 61.04%, while CaO achieved only 14.53%. This improvement under UV light highlighted the photocatalytic activity of the CaO-ZnO biocomposite, which significantly contributed to the degradation process. The biocomposite of CaO-ZnO exhibited higher enrofloxacin removal efficiency under UV irradiation

compared to CaO due to the synergistic effect of ZnO's photocatalytic properties. ZnO acted as a photocatalyst, generating reactive oxygen species (ROS), such as hydroxyl radicals (•OH) and superoxide anions (•O_2^-), when exposed to UV light [34, 35]. These ROS are highly reactive and effectively degraded organic pollutants, such as tetracycline. In contrast, CaO primarily functioned as an adsorbent and lacked significant photocatalytic activity. Overall, the CaO-ZnO biocomposite demonstrated superior performance compared to CaO in removing enrofloxacin, particularly under UV irradiation, making it a promising material for water treatment applications.
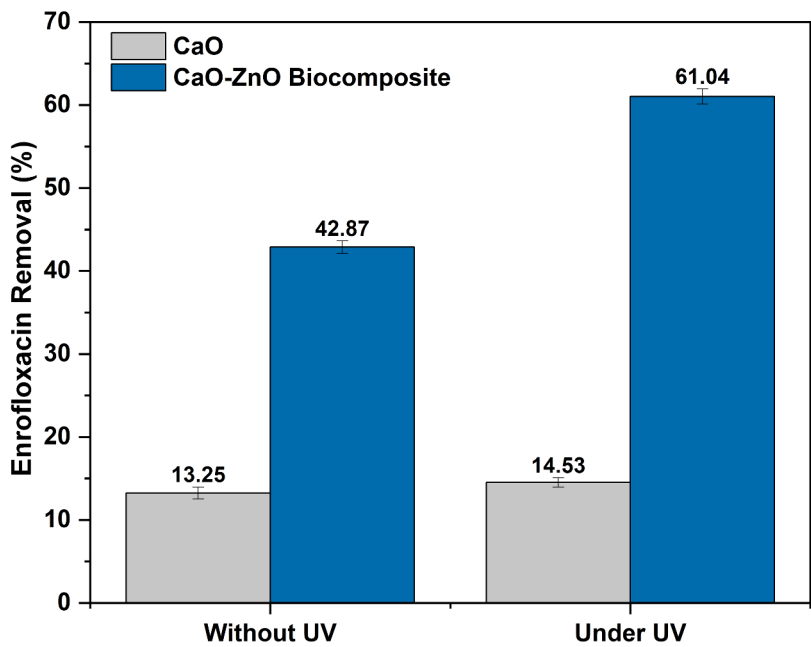

Fig. 5. Enrofloxacin removal using CaO and CaO-ZnO biocomposites without and under UV light irradiation.

4 Conclusion

The oyster shell-derived CaO-ZnO composite demonstrated better performance than CaO in removing enrofloxacin from water, especially under UV irradiation, achieving a removal efficiency of 61.04% compared to 14.53% for CaO. This improvement is attributed to the photocatalytic properties of ZnO, which enhanced the degradation of enrofloxacin. The best performance was observed at pH 3 due to favorable electrostatic interactions. These results highlight the potential of CaO-ZnO composites as an efficient and sustainable material for addressing antibiotic contamination in water systems. Further parameter optimization is recommended to enhance their performance.

Acknowledgment

References

1. J. Fučík, A. Amrichová, K. Brabcová, R. Karpíšková, I. Koláčková, L. Pokludová, S. Poláková, L. Mravcová, Fate of fluoroquinolones in field soil environment after incorporation of poultry litter from a farm with enrofloxacin administration via drinking water. Environmental Science and Pollution Research. **31**, 20017-20032 (2024)

2. F. Xi, The enrofloxacin pollution control from fish to environment. Marine Pollution Bulletin. **199**, 115923 (2024)

3. B. S. Vorbach, J. Zhou, Y. Lang, J. B. Bulitta, R. P. Yanong, Population pharmacokinetics of enrofloxacin and florfenicol in the giant danio (Devario aequipinnatus) following oral administration of both antibiotics and bath administration of enrofloxacin. Aquaculture. **579**, 740222 (2024)

4. T. Z. Addis, J. T. Adu, M. Kumarasamy, M. Demlie, Occurrence of Trace-Level Antibiotics in the Msunduzi River: An Investigation into South African Environmental Pollution. Antibiotics. **13**, 174 (2024)

5. M.M. Selim, A. Tounsi, H. Gomaa, N. Hu, M. Shenashen, Addressing emerging contaminants in wastewater: Insights from adsorption isotherms and adsorbents: A comprehensive review. Alexandria Engineering Journal. **100**, 61-71 (2024)

6. I. Salahshoori, Q. Wang, M.A. Nobre, A.H. Mohammadi, E.A. Dawi, H.A. Khonakdar, Molecular simulation-based insights into dye pollutant adsorption: a perspective review. Advances in Colloid and Interface Science. **333**, 103281 (2024).

7. B.S. Rathi, P.S. Kumar, Application of adsorption process for effective removal of emerging contaminants from water and wastewater. Environmental Pollution. **280**, 116995 (2021)

8. M.S. Akhtar, S. Ali, W. Zaman, Innovative adsorbents for pollutant removal: Exploring the latest research and applications. Molecules. **29(18)**, 4317 (2024)

9. V. Prajaputra, S. Karina, A. Bismi, P. H. Nuufus, The removal of ciprofloxacin from water by Alue Naga and Leungah beach sand. IOP Conference Series: Earth and Environmental Science. **1356**, 012058 (2024)

10. A. G. Fahmi, Z. Abidin, C. Kusmana, D. Kharisma, V. Prajaputra, W. R. Rahmawati, Preparation and characterization of activated carbon from palm kernel shell at low temperature as an adsorbent for methylene blue. IOP conference series: earth and environmental science. **399**, 012015 (2019)

11. V. Saadattalab, J. Wu, C.W. Tai, Z. Bacsik, N. Hedin, Adsorption of volatile organic compounds on activated carbon with included iron phosphate. Carbon Trends. **11**, 100259 (2023)

12. V. Prajaputra, Z. Abidin, Widiatmaka, Methylene Blue Removal Using Developed Material from Volcanic Ash Soils. International Journal of Scientific & Technology Research. **8**, 706-709 (2019)

13. R. Lavecchia, A. Zuorro, O. Baaloudj, M. Brienza, Trimethoprim removal from aqueous solutions via volcanic ash-soil adsorption: process modeling and optimization. Water, **16(15)**, 2209 (2024)

14. V. Prajaputra, Z. Abidin, S. Budiarti, D. T. Suryaningtyas, N. Isnaini, Comparative study of methylene blue adsorption using alkali-activated pumice from Bali and Banten. Journal of Physics: Conference Series. **1882**, 012118 (2021)

15. K. Güneş, Isotherm and kinetic modeling of the adsorption of methylene blue, a cationic dye, on pumice. International Journal of Chemistry and Technology. **7(1)**, 67-74 (2023)

16. V. Prajaputra, Z. Abidin, S. Budiarti, D. T. Suryaningtyas, Synergistic effect of adsorption and Fenton-like oxidation processes for Methylene blue removal using Na-P1 zeolite prepared from pumice. Desalination and Water Treatment. **218**, 401-408 (2021)

17. Z.A. Hammood, T.F. Chyad, R. Al-Saedi, Adsorption performance of dyes over zeolite for textile wastewater treatment. Ecological Chemistry and Engineering S. **28(3)**, 329-337 (2021)

18. I.O. Saheed, W. Da Oh, F.B.M. Suah, Chitosan modifications for adsorption of pollutants–A review. Journal of hazardous materials. **408**, 124889 (2021)

19. P. Sirajudheen, N.C. Poovathumkuzhi, S. Vigneshwaran, B.M. Chelaveettil, S. Meenakshi, Applications of chitin and chitosan based biomaterials for the adsorptive removal of textile dyes from water—A comprehensive review. Carbohydrate polymers. **273**, 118604 (2021)

20. S. Karina, V. Prajaputra, A.W. Perdana, N. Isnaini, A. Bismi, P.H. Nuufus, Removal of tetracycline from aqueous solution by beach sand-based silica. IOP Conference Series: Earth and Environmental Science. **1266**. 012034 (2023)

21. S.S. Batool, Z. Imran, S. Hassan, K. Rasool, M. Ahmad, M.A. Rafiq, Enhanced adsorptive removal of toxic dyes using SiO2 nanofibers. Solid State Sciences. **55**, 13-20 (2016)

22. S. Karina, A. W. Perdana, V. Prajaputra, N. Isnaini, P. H. Nuufus, A. Bismi, Silica-Magnetite Composite as an Eco-Friendly Adsorbent for Aqueous Tetracycline Removal–Kinetic and Isotherm Studies. Ecological Engineering & Environmental Technology. **25**, 82-92 (2024)

23. F. Keyhanian, S. Shariati, M. Faraji, M. Hesabi, Magnetite nanoparticles with surface modification for removal of methyl violet from aqueous solutions. Arabian Journal of Chemistry. **9**, S348-S354 (2016)

24. S. Lubis, Sheilatina, S.S. Nika, V.P. Putra, Adsorption of naphthol blue black dye onto acid activated titania pillared bentonite: Equilibrium study. Oriental Journal of Chemistry. **32**, 1789-97 (2016)

25. C. Leodopoulos, D. Doulia, K. Gimouhopoulos, Adsorption of cationic dyes onto bentonite. Separation & Purification Reviews. **44(1)**, 74-107 (2015)

26. Z. Abidin, B. Syamsi, S. Sugiarti, S. Murtini, D. Kharisma, V. Prajaputra, A. G. Fahmi, Synthesis of Magnetite/Volcanic Soil Composite from West of Java and Its Adsorption Properties. IOP Conference Series: Earth and Environmental Science. **187**, 012075 (2018)

27. V. Prajaputra, S. Karina, N. Isnaini, P.S. Rahayu, M. Sihombing, Investigating the potential of coral fragment-based CaO-ZnO biocomposites for the sustainable photodegradation of chloramphenicol. Ecological Engineering & Environmental Technology. **26(2)**, 420-427 (2025)

28. A.O. Adeleke, R.C. Omar, K.K. Katibi, T.T. Dele-Afolabi, A. Ahmad, J.O. Quazim, A.A. Amusa, M.B. Alshammari, Process optimization of superior biosorption capacity of biogenic oyster shells nanoparticles for Congo red and Bromothymol blue dyes removal from aqueous solution: Response surface methodology, equilibrium isotherm, kinetic, and reusability studies. Alexandria Engineering Journal. **92**, 11-23 (2024)

29. W. Song, Y. Zeng, J. Wu, Q. Huang, R. Cui, D. Wang, Y. Zhang, M. Xie, D. Feng, Effects of oyster shells on maturity and calcium activation in organic solid waste compost. Chemosphere. **345**, 140505 (2023)

30. J. Zhang, B. Zheng, C. Zhang, L. Xie, C. Fang, J. Zhang, B. Zheng, C. Zhang, L. Xie, C. Fang, Calcined waste shells as a promising, eco-friendly adsorbent, antimicrobial, food preservative, and food packaging material: A mini review. Journal of Food Process Engineering. **46**, e14477 (2023)

31. J. Rodrigues, N. B. Sedrine, M.R. Correia, T. Monteiro, Photoluminescence investigations of ZnO micro/nanostructures. Materials Today Chemistry. **16**, 100243 (2020)

32. Y. Zhang, W. Yang, Z. Zhu, L. Zhang, W. Peng, Temperature-Sensitive Template for Preparation of ZnO/CeO2 Composite Photocatalytic Materials and Its Catalytic Performance. Molecules. **29**, 3589 (2024)

33. N. Sazali, Z. Harun, N. Sazali, A review on batch and column adsorption of various adsorbent towards the removal of heavy metal. Journal of Advanced Research in Fluid Mechanics and Thermal Sciences. **67(2)**, 66-88 (2020)

34. Y. Sun, W. Zhang, Q. Li, H. Liu, X. Wang, Preparations and applications of zinc oxide based photocatalytic materials. Advanced Sensor and Energy Materials. **2(3)**, 100069 (2023)

35. Z.A. Pollard, M. Karod, A. Schmitz, B. Pian, B. Barstow, J.L. Goldfarb, ZnO Precursor's ability to catalyze formation of reactive oxygen species to degrade aqueous organic pollutants. Chemical Engineering Journal. **480**, 147499 (2024)